Chinese Journal of Physics 87 (2024) 246–255

Contents lists available at ScienceDirect

Chinese Journal of Physics

journal homepage: www.elsevier.com/locate/cjph

Effects of coupling on extremely multistable fractional-order systems

Karthikeyan Rajagopal [a], Fatemeh Parastesh [a], Hamid Reza Abdolmohammadi [b], Sajad Jafari [c,d], Matjaž Perc [e,f,g,*], Eva Klemenčič [e,h]

[a] Centre for Nonlinear Systems, Chennai Institute of Technology, Chennai, 600069, Tamil Nadu, India
[b] Electrical and Computer Engineering Group, Golpayegan College of Engineering, Isfahan University of Technology, Golpayegan, 87717-67498, Iran
[c] Department of Biomedical Engineering, Amirkabir University of Technology, Tehran, 1591634311, Iran
[d] Health Technology Research Institute, Amirkabir University of Technology, Tehran, 1591634311, Iran
[e] Faculty of Natural Sciences and Mathematics, University of Maribor, Koroška cesta 160, 2000 Maribor, Slovenia
[f] Complexity Science Hub Vienna, Josefstädterstraße 39, 1080 Vienna, Austria
[g] Department of Physics, Kyung Hee University, 26 Kyungheedae-ro, Dongdaemun-gu, Seoul, Republic of Korea
[h] Faculty of Energy Technology, University of Maribor, Hočevarjev trg 1, 8270 Krško, Slovenia

ARTICLE INFO

Keywords:
Fractional-order
Extreme multistability
Neural network model
Coupling

ABSTRACT

Multistability is a phenomenon in which a dynamical system possesses multiple attractors within the same set of parameters. This study explores the effects of coupling on the dynamics of a recently introduced 2D single-neuron neural network model. The system is in its original form bistable, but its extension to include fractional-order derivatives yields an unprecedented level of complexity that is characterized by extreme multistability. We provide a comprehensive analysis of the behavior of this system when coupled. We find a diverse range of attractors for two coupled systems emerging from different initial conditions, and we elucidate the transition from periodic to chaotic behavior as the coupling strength increases. We also show that the synchronization dynamics in this case ranges from anti-phase synchronization under weak coupling to complete synchronization under stronger coupling. Finally, we study the collective behavior of several coupled extremely multistable fractional-order systems, which compared to bistable systems exhibit more complexity and uncertainty as they oscillate between different attractors, or even between emerging attractors.

1. Introduction

The concept of collective dynamics in complex networks belongs to the emergence of patterns or behaviors resulting from interactions among individual nodes within a network [1,2]. This phenomenon can be observed across various systems, including social, biological, and technological networks [3–5]. Various behaviors, such as the formation of clusters, the emergence of interesting patterns, and the synchronization of nodes, are known as the collective behavior of networks [6–8]. Numerous studies have tried to analyze these behaviors in different networks [9–12]. In addition to the emergence of collective patterns, the impacts of the interactions on the dynamics of the nodes possess special significance in diverse applications, including assessing the systems' function and their manipulation or control.

* Corresponding author at: Faculty of Natural Sciences and Mathematics, University of Maribor, Koroška cesta 160, 2000 Maribor, Slovenia.
E-mail address: matjaz.perc@gmail.com (M. Perc).

https://doi.org/10.1016/j.cjph.2023.12.011
Received 9 November 2023; Received in revised form 5 December 2023; Accepted 7 December 2023
Available online 10 December 2023

In dynamical systems, the concept of multistability presents an intriguing characteristic where a single system can manifest multiple stable states or attractors [13]. This feature leads to the formation of a diverse and complicated range of possible behaviors. In a multistable system, the system can possess two or more stable states or attractors with distinct properties. Extreme multistability takes the concept of multistability to a higher degree of complexity [14]. Systems exhibiting extreme multistability can adopt many stable states or attractors [15]. This infrequent feature usually causes unpredictable and complicated dynamics. Extreme multistability may emerge due to a large number of variables, intricate interactions, or feedback mechanisms. Multistability and extreme multistability find applications in various fields, including neuroscience, control theory, and the modeling of economic systems [16–19]. Bao et al. [20] represented the emergence of extreme multistability in a memristive Chua's circuit.

In the field of modeling dynamical systems, fractional-order derivative has served as a valuable tool [21]. Fractional-order derivatives, as introduced through fractional calculus, represent a generalization of the conventional differentiation concept using non-integer or fractional values. Fractional-order derivatives incorporate the memory effect [22]; hence, the states of a system are influenced by their prior states over a range of time. Fractional calculus has various applications in various fields, including dynamical systems, electrochemistry, control theory, biology, and finance [23–26]. In recent years, a great deal of research has been devoted to investigating systems with fractional orders [27–31].

In the past years, a great effort has been devoted to study of neural network models [32–34]. The reason is that they offer powerful tools for solving a wide range of problems across various domains such as pattern recognition, computer vision, classification, etc. [35,36]. Among various neural network models, the Hopfield neural network (HNN) has been of greater interest and used for different tasks. Subsequently, various HNN models have been presented with different properties [37–39]. Recently, the simplest neural network model with one neuron and memristor was proposed [40]. This paper investigates the network of this model with complex behaviors considering fractional-order derivatives [41]. The specific ability of this model is to have many different attractors depending on the initial condition in some fractional orders. The aim is to explore how the dynamics and attractors of systems change when multiple such systems are coupled. By studying these systems, researchers can uncover unexpected behaviors and patterns that emerge from individuals' interactions. Detecting the influence of coupling on these systems can have practical applications in predicting and managing their behavior and even presenting control strategies. Hence, it can help understand the behavior of complex systems in various natural and engineered fields. An example is the behavior of neural networks and the brain. The brain is a highly interconnected network of neurons, and realizing the effects of coupling on multistable systems provides significant information about the communication of different brain regions.

Here, it is found that under weak connections, two coupled systems produce regular patterns, which are turned to chaotic with stronger connections. In addition, these systems are synchronized differently under varying initial conditions. The study is then extended to a ring of such systems, and interesting behaviors are observed, including the emergence of new attractors. The fractional neural model is described in Section 2. The dynamics of two coupled systems and the ring of coupled systems are explored in Sections 3 and 4, respectively. Finally, the conclusions are provided in Section 5.

2. Fractional-order model

In 2022, Hua et al. [40] presented the simplest neural network model consisting of a single neuron with memristive synaptic weights. The general equations describing the dynamics of neuron i in a Hopfield neural network is as follows,

$$C_i \frac{dx_i}{dt} = \frac{-1}{R_i} x_i + \sum_j w_{ij} Y_j + I_i, \tag{1}$$

where x_i, $C_i = 1$, and $R_i = 1$ are the membrane potential, capacitance, and resistance of the neuron. The weight of the synaptic connection from the j-th neuron to i-th neuron is shown by w_{ij}. Hua et al. considered a single neuron model with a memristive connection weight considering a memductance function as $W(\phi) = \phi^2 - 0.5$. Hence, they presented the following model,

$$\begin{aligned} \dot{x} &= -x + kW(\phi)g(x) + I, \\ \dot{\phi} &= g(x) - 2\phi, \end{aligned} \tag{2}$$

where x is the membrane potential, ϕ is the inner state of the memristor, $I = A\sin(2\pi F t)$ is the excitation current with amplitude $A = 3$ and frequency $F = 1$. The parameter k is set to $k = 4$. The nonlinear activation function is defined as $g(x) = \tanh(2x - 3) + \tanh(2x + 3) - 2\tanh(2x)$. As shown in [40], this simple model is multistable and capable of exhibiting rich dynamics.

Recently, Sriram et al. [41] studied this model by considering fractional-order derivatives, as follows,

$$\begin{aligned} D^q x &= -x + kW(\phi)g(x) + I, \\ D^q \phi &= g(x) - 2\phi, \end{aligned} \tag{3}$$

where D^q denotes the Caputo derivative. It is defined as

$$\begin{cases} D_t^q f(t) = \frac{1}{\Gamma(m-q)} \int_0^t f^{(m)}(\tau)(t-\tau)^{m-q-1} d\tau, & \text{if } m-1 < q < m, \\ D_t^q f(t) = f^{(m)}(t), & \text{if } q = m, \end{cases} \tag{4}$$

where Γ is the gamma function. To solve the fractional-order equations, the predictor–corrector method is applied [42].

Sriram et al. interestingly found that the fractional-order derivatives lead to the emergence of extreme multistability. Moreover, in contrast to most extreme multistable systems in which the multistability depends on the initial condition of only one variable, here, both initial conditions cause extreme multistability. The bifurcation diagrams of the model, as the maximum value of x variable

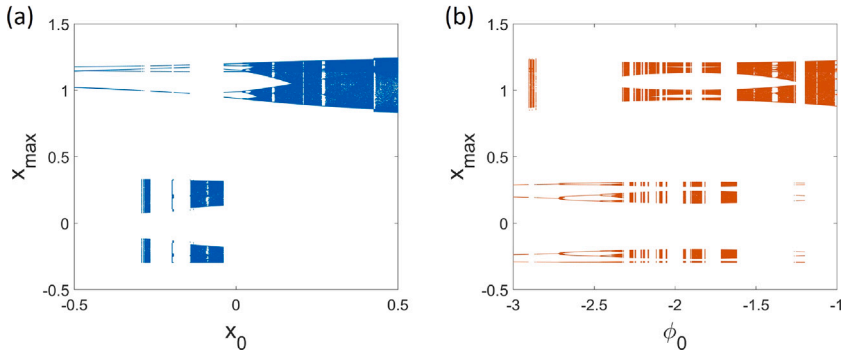

Fig. 1. Bifurcation diagram of the single model with fractional derivative $q = 0.96$ versus the initial condition of x variable in (a) where $\phi_0 = 4$, and versus the initial condition of ϕ variable in (b) where $x_0 = 1$. Varying the initial conditions lead to infinite attractors, making the model extreme multistable.

for $q = 0.96$ with respect to the initial conditions, are shown in Fig. 1. In Fig. 1(a), $\phi_0 = 4$ and in Fig. 1(b), $x_0 = 1$ is set. It can be observed that the system can show various periodic and chaotic dynamics according to the initial conditions. Furthermore, the attractors are located in two groups of $\phi < 0$ and $\phi > 0$, referred to as negative and positive groups in the following.

The equilibrium point of the model has been provided in [40] as Eq $= [\mu, 0.5g(\mu)]$, where μ satisfies the following equation,

$$H(\mu) = \mu - 0.25k[g^2(\mu) - 2]g(\mu) - I. \tag{5}$$

Hence, the equilibrium point is periodically variable, and depends on the excitation current. For the stability analysis, the eigenvalues of the Jacobian matrix of the systems must be found, which are as follows,

$$J = \begin{bmatrix} -1 - 0.25k[g^2(\mu) - 2]g'(\mu) & kg^2(\mu) \\ g'(\mu) & -2 \end{bmatrix}. \tag{6}$$

By defining a and b as follows,

$$\begin{aligned} a &= 3 - 0.25k[g^2(\mu) - 2]g'(\mu), \\ b &= 2 - k[1.5g^2(\mu) - 1]g'(\mu), \end{aligned} \tag{7}$$

the eigenvalues can be found as, $\lambda_{1,2} = -0.5a \pm 0.5\sqrt{a^2 - 4b}$. For a fractional order model, the equilibrium point is stable if $|\arg(\lambda)| < q\pi/2$, where arg denotes the principal argument. For $a^2 - 4b > 0$, $\arg(\lambda) = 0$, and therefore, the equilibrium point is unstable. For $a^2 - 4b < 0$, there are a complex conjugate pair of eigenvalues as $\lambda_{1,2} = \alpha \pm j\beta$. Hence, $|\arg(\lambda)| = |\beta/\alpha| = |\sqrt{a^2 - 4b}/a|$. If $|\sqrt{a^2 - 4b}/a| > q\pi/2$, the equilibrium point is stable. Solving this equation leads to the condition $b > (q\pi/2 + 1)a^2/4$.

3. Bi-neuron network

Firstly, the behavior of the two coupled systems is studied. Two coupled fractional-order models can be described by,

$$\begin{aligned} D^q x_1 &= -x_1 + kW(\phi_1)g(x_1) + I + \sigma(x_2 - x_1), \\ D^q \phi_1 &= g(x_1) - 2\phi_1, \\ D^q x_2 &= -x_2 + kW(\phi_2)g(x_2) + I + \sigma(x_1 - x_2), \\ D^q \phi_2 &= g(x_2) - 2\phi_2, \end{aligned} \tag{8}$$

with σ showing the strength of coupling between two systems and $0 < q \leq 1$. As an example for the fractional order, we choose $q = 0.96$. As shown in the bifurcation diagrams in Fig. 1, the system shows different periodic and chaotic attractors. It is notable that the 0–1 test was used to detect the chaotic dynamics [43]. Hence, we consider different sets of initial conditions for two systems and increase the coupling strength to find how the attractors change. In this regard, four different initial conditions are considered as,

Case A. $(x_1(0), \phi_1(0), x_2(0), \phi_2(0)) = (0.1, 4, -0.1, 4)$: The uncoupled systems have chaotic attractors, one in the negative group and another in the positive group.

Case B. $(x_1(0), \phi_1(0), x_2(0), \phi_2(0)) = (-0.1, 4, -0.5, 4)$: The uncoupled systems have a chaotic attractor in the positive group and a periodic attractor in the negative group.

Case C. $(x_1(0), \phi_1(0), x_2(0), \phi_2(0)) = (1, 4, 2, 4)$: The uncoupled systems have two different chaotic attractors in the negative group.

Case D. $(x_1(0), \phi_1(0), x_2(0), \phi_2(0)) = (-2, -4, 2, -4)$: The uncoupled systems have two different chaotic attractors in the positive group.

The attractors of the uncoupled systems (dark and light blue colors) for four defined cases are shown in the left column of Fig. 2. The corresponding time series of Fig. 2 are illustrated in Fig. 3 with dark and light green colors. When the systems have two chaotic

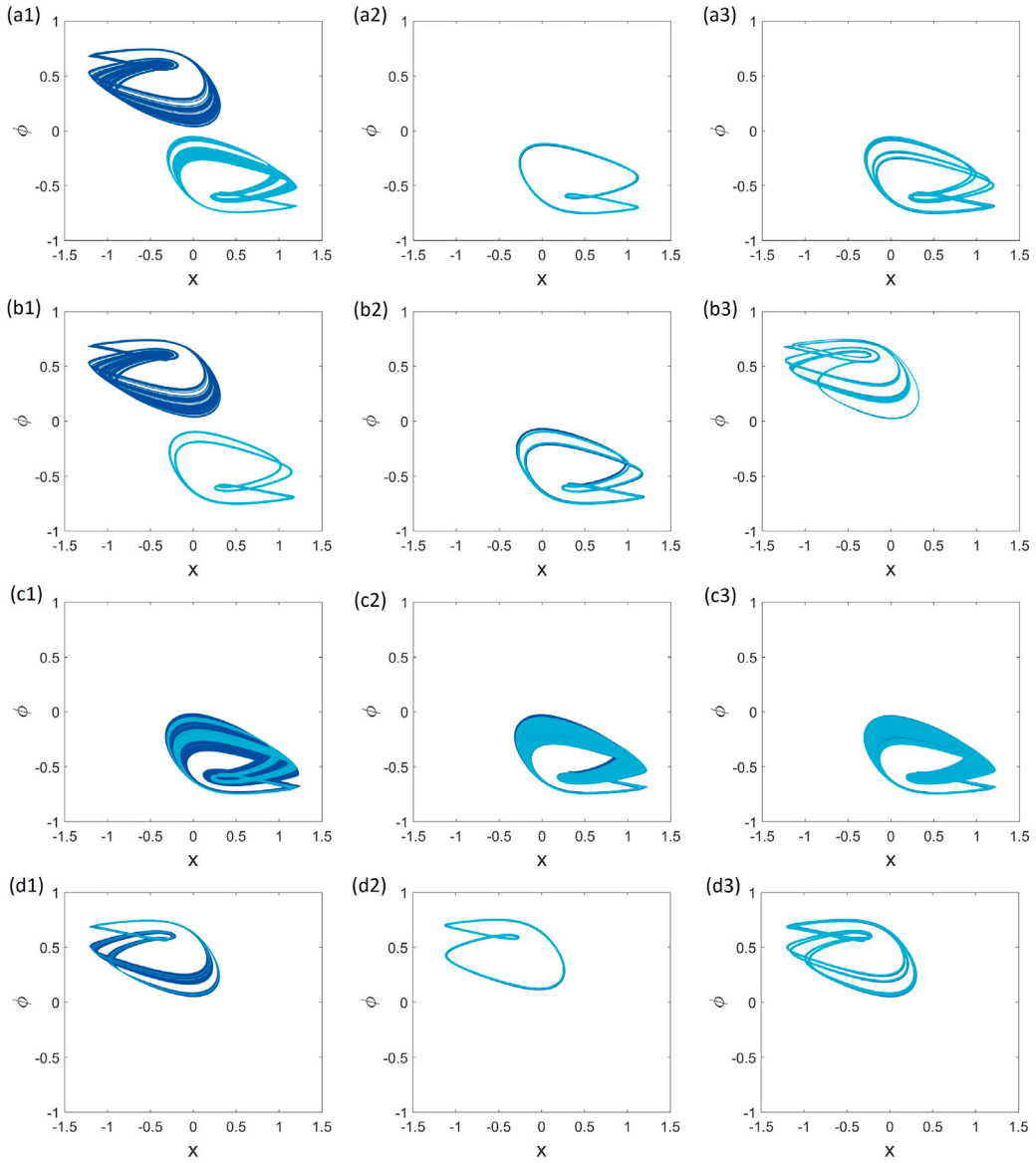

Fig. 2. The attractors of fractional-order bi-neuron network with $q = 0.96$. The attractors of two systems are shown by light and dark blue colors. In the left column, the systems are uncoupled; in the middle panel, the coupling is weak; in the right panel, the coupling is strong. The initial conditions $(x_1(0), \phi_1(0), x_2(0), \phi_2(0))$ are (a) $(0.1, 4, -0.1, 4)$, (b) $(-0.1, 4, -0.5, 4)$, (c) $(1, 4, 2, 4)$, (d) $(-2, -4, 2, -4)$. This figure represents the transition between different attractors due to the coupling strength. (For interpretation of the references to color in this figure legend, the reader is referred to the web version of this article.)

attractors in two groups (Fig. 2(a1)), a slight increase in the coupling strength leads to the conversion of chaotic attractors to period-2 attractor, locating in the negative group (Fig. 2(a2)). The time series shown in Fig. 3(a2) represents that the systems are anti-phase synchronous in this case. In this state, the phase of two systems is in opposite. In other words, the systems can be synchronous by a phase shift. By more increasing the coupling strength, the systems reach a complete synchronous state with period-6 oscillations (Figs. 2(a3) and 3(a3)). If the systems initiate from a chaotic and a periodic attractor, as shown in Fig. 2(b1), a semi-synchronous periodic state is formed in the negative group in low couplings (Fig. 2(b2)). Then, as coupling grows, a chaotic synchronous state emerges in the positive location (Fig. 2(b3)). In the next case, when both attractors are chaotic and in the negative group (Fig. 2(c1)), strengthening the coupling keeps the chaotic attractors, and they remain in the negative group (Fig. 2(c2) and (c3)). Finally, when the uncoupled systems have two chaotic attractors in the positive groups, in lower coupling strengths, an anti-phase synchronous state is formed. The corresponding time series can be observed in Fig. 3(d2). When the coupling becomes stronger, a period-5 synchronization is achieved (Figs. 2(d3) and 3(d3)).

To have a more complete view of the behavior of two coupled fractional-order systems, 2D bifurcation diagrams are obtained according to the coupling strength for different fractional orders. To investigate the effect of the initial conditions, three cases ((A),

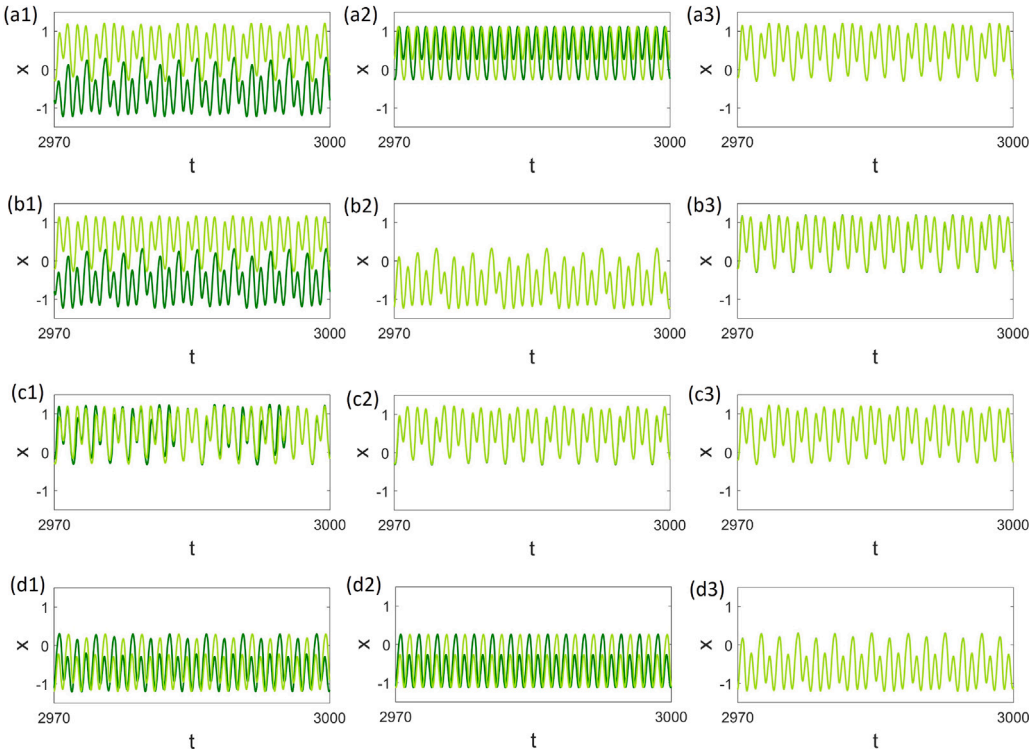

Fig. 3. The time series of fractional-order bi-neuron network corresponding to Fig. 2. The time series of two systems are shown by light and dark green colors. When the initial states of two systems are in the same phase space region, the coupled systems remain in that region. Parts (a2) and (d2) show anti-phase synchronization. (For interpretation of the references to color in this figure legend, the reader is referred to the web version of this article.)

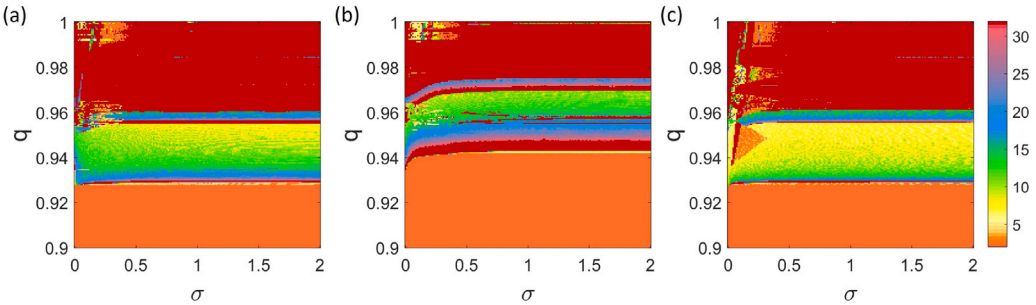

Fig. 4. 2D bifurcation diagrams of the bi-neuron network with respect to the fractional order (q) and coupling strength (σ). The color bar shows the period of oscillations. The initial conditions $(x_1(0), \phi_1(0), x_2(0), \phi_2(0))$ are (a) $(0.1, 4, -0.1, 4)$, (b) $(-0.1, 4, -0.5, 4)$, (c) $(-2, -4, 2, -4)$. The coupling affects the systems' dynamics more in the lower coupling strengths and higher fractional orders. In higher fractional orders, periodic attractors are formed in weak coupling and choatic attractors are formed in strong coupling. (For interpretation of the references to color in this figure legend, the reader is referred to the web version of this article.)

(B) and (D) defined above) are chosen. The results are shown in Fig. 4, where the period of oscillations is shown by color. Note that the periods above 32 are set to 32 and considered chaotic dynamics. Comparing three bifurcation diagrams indicates that in case B, where initial attractors are periodic and chaotic, the periodic region is larger (the chaotic region is smaller) than in two other cases, where two initial attractors are chaotic. Moreover, in case B, there is a chaotic region in the range of $q = 0.94$, which is not observed in two other cases. The effect of the coupling strength on the attractors occurs more in the weak couplings. Furthermore, in case C, the change in the attractors happens for more values of q. When the coupling strength is small, the attractors are periodic, and as the coupling becomes stronger, the attractors change to chaotic.

Besides the dynamics of coupled systems, their synchronization is of great importance. We measure the complete synchronization of the bi-neuron network by computing the complete synchronization error as follows,

$$E = \langle \sqrt{(x_1 - x_2)^2 + (\phi_1 - \phi_2)^2} \rangle_t, \tag{9}$$

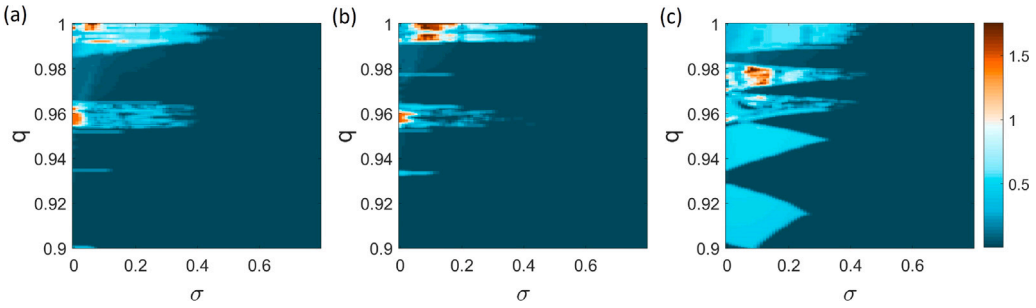

Fig. 5. Synchronization error of the bi-neuron network with respect to the fractional order (q) and coupling strength (σ). The initial conditions $(x_1(0), \phi_1(0), x_2(0), \phi_2(0))$ are (a) (0.1,4,−0.1,4), (b) (−0.1,4,−0.5,4), (c) (−2,−4,2,−4). The dark color represents the synchronization region. It is evident that the synchronization in extreme multistable systems is dependent on the initial conditions. For some initial conditions as part (c), two systems reach anti-phase synchronization in weaker couplings, and hence, complete synchronization region becomes smaller. (For interpretation of the references to color in this figure legend, the reader is referred to the web version of this article.)

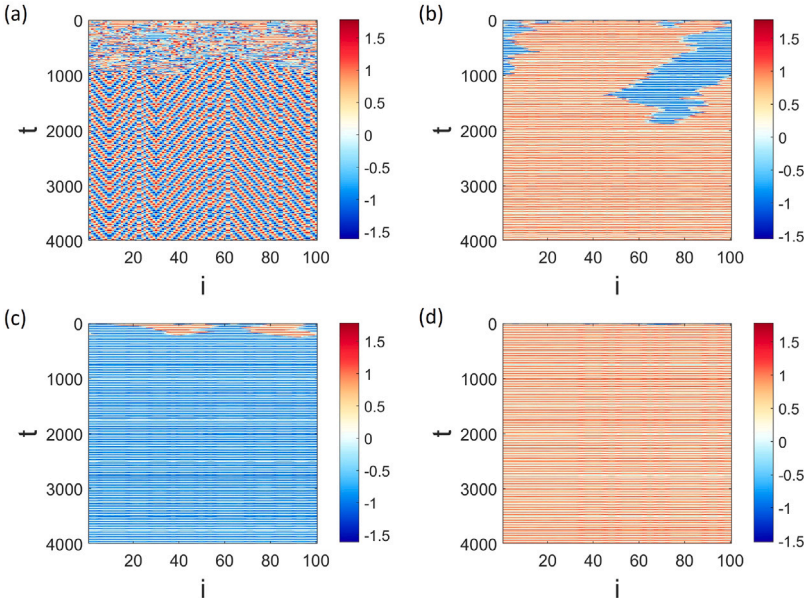

Fig. 6. Spatiotemporal patterns of the ring network of fractional-order systems with $q = 0.96$ for which the system is extreme multistable. (a) $\sigma = 0.1$, (b) $\sigma = 0.3$, (c) $\sigma = 0.5$, (d) $\sigma = 1.2$. In weak coupling, the systems move between attractors in two groups and stay in two groups. In stronger couplings, the systems are attracted to one group after transient.

with $\langle\rangle_t$ representing time average. Fig. 5 shows the complete synchronization error with respect to the fractional order and coupling strength. The dark regions depict the complete synchronous state. Three subfigures refer to three different initial conditions ((A), (B) and (C) defined above). Comparing three cases shows that the synchronization region is dependent on the initial condition of the systems. In case A and B, the synchronization regions are almost similar. However, this region is a bit larger in case B, in which one system has originally periodic attractor. Case C has a smaller synchronization region. The reason is that for these initial conditions, the systems become almost anti-phase synchronous for lower couplings. It is notable that reaching synchronization in the context of neural networks represents an energy balance that refers to the equilibrium between the energy consumed and the energy produced systems [44]. Achieving energy balance is essential for the proper functioning and sustainability of the systems.

4. Ring network

In this section, the aim is to study the dynamics when more neurons are coupled. Hence, a ring structure with 100 neural models is considered as follows,

$$\begin{aligned} D^q x_i &= -x_i + kW(\phi_i)g(x_i) + I + \sigma(x_{i-1} + x_{i+1} - 2x_i), \\ D^q \phi_i &= g(x_i) - 2\phi_i. \end{aligned} \tag{10}$$

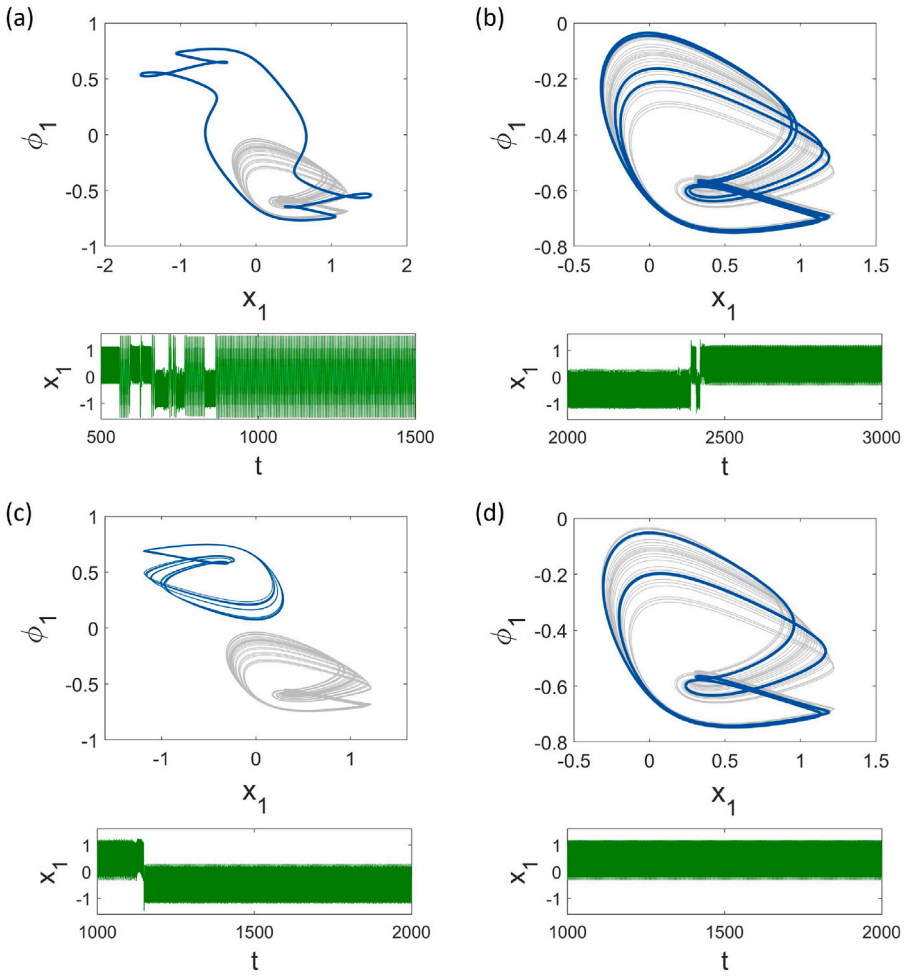

Fig. 7. The attractor and the time series of the first neuron of the network corresponding to Fig. 6. (a) $\sigma = 0.1$, (b) $\sigma = 0.3$, (c) $\sigma = 0.5$, (d) $\sigma = 1.2$. The gray color shows the attractor in the absence of coupling. Formation of a new attractor is shown in part (a) where the coupling is weak. In stronger couplings, the systems are attracted to one of attractors groups. (For interpretation of the references to color in this figure legend, the reader is referred to the web version of this article.)

The initial conditions of the x variables of neurons are selected randomly in the range $[-0.5, 0.5]$ and ϕ variables are set at 4. Firstly, we examine $q = 0.96$, for which the system is extremely multistable; hence, for the chosen random initial conditions, the uncoupled systems have different chaotic and periodic attractors according to Fig. 1(a). The spatiotemporal patterns of the network for different coupling strengths are shown in Fig. 6. In Fig. 6(a), where the coupling is $\sigma = 0.1$, the network is asynchronous. The time series and attractor of the first system of the network are shown in Fig. 7(a) as an example. The attractors before coupling and after coupling are illustrated in gray and blue colors, respectively. It can be observed that coupling first makes the systems move between two groups of attractors. Then, as time passes, systems reach a new periodic attractor, which is composed of two groups. As the coupling becomes stronger, the systems move between the attractors in the transient time and then are attracted to one of them. The spatiotemporal patterns of this coupling are shown in Fig. 6(b),(c). The corresponding attractor and time series of the first neuron are illustrated in Fig. 7(b),(c). For $\sigma = 0.3$, the systems are attracted to the chaotic attractor in the negative group and for $\sigma = 0.5$, the chaotic attractor in the positive group is dominant. Finally, by increasing the coupling, the systems become synchronous in a periodic attractor, as shown in Figs. 6(d) and 7(d).

In the next step, the network is investigated for $q = 0.98$, in which the fractional-order system is bistable. The spatiotemporal patterns for weak and strong couplings are shown in Fig. 8, and the time series and attractor of the first neuron is demonstrated in Fig. 9. In this case, in contrast to $q = 0.96$, the systems do not move between positive and negative groups. Also, no new attractor is formed. In weak coupling, the network is asynchronous; some of the systems have positive attractors, and some have negative attractors. In strong coupling, the network becomes synchronous in one of the attractors.

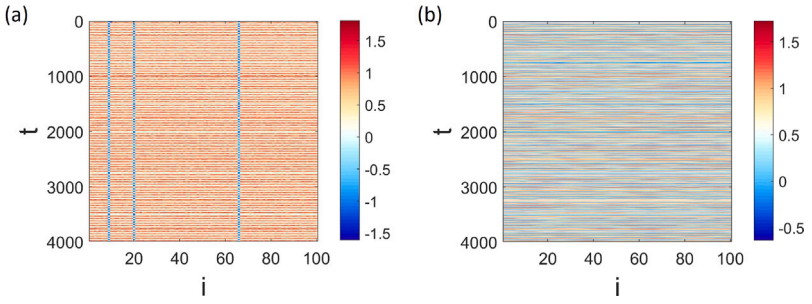

Fig. 8. Spatiotemporal patterns of the ring network of fractional-order systems with $q = 0.98$ for which the system is bistable. (a) $\sigma = 0.05$, (b) $\sigma = 1.2$. In weak coupling, the systems oscillate in either the positive attractor or the negative attractor. In stronger couplings, the systems are attracted to one attractor.

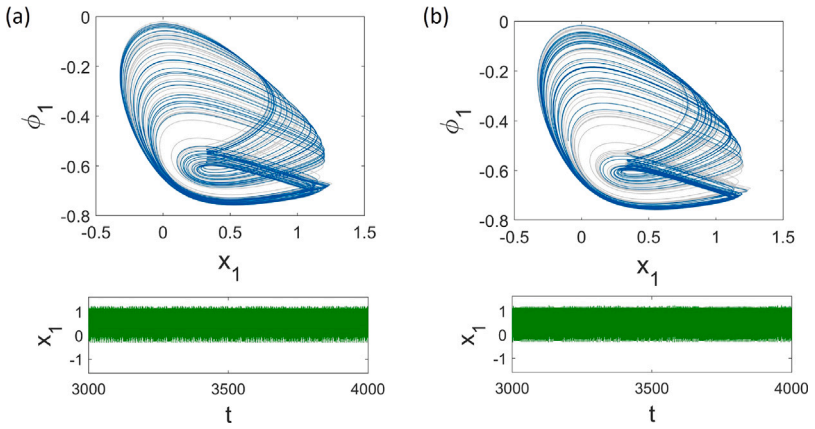

Fig. 9. The attractor and the time series of the first neuron of the network corresponding to Fig. 8. (a) $\sigma = 0.05$, (b) $\sigma = 1.2$. The gray color shows the attractor in the absence of coupling. In this case, no new attractor is formed. (For interpretation of the references to color in this figure legend, the reader is referred to the web version of this article.)

5. Conclusion

In summary, this study presents an exploration of the dynamics of a recently introduced memristive single-neuron neural network model with bistability. The extension of this model to incorporate fractional-order derivatives has resulted in extreme multistability, representing an unprecedented level of multistability for a 2D model. To be more specific, the fractional-order model has many attractors both in the positive and negative memristive variable regions. While prior research has primarily focused on networks of monostable or bistable systems characterized by one or two attractors, this paper extended the analysis to systems exhibiting extreme multistability. By examining the dynamics of two coupled fractional-order systems under specific conditions, it was demonstrated that under weak couplings, the systems primarily exhibit periodic attractors. As the coupling strength increases, the transition to chaotic behavior occurs. In addition, the paper highlighted the synchronous behavior of the coupled systems, shifting from anti-phase synchronization in weak couplings to complete synchronization in stronger coupling regimes.

The investigation was further extended to ring networks, providing insights into the collective behavior of multiple extreme multistable systems. In very weak couplings, the systems oscillated between distinct groups of attractors, eventually converging into a unified attractor composed of both positive and negative attractors. With stronger couplings, the systems exhibited synchronized behavior within one specific attractor group. Compared to extreme multistability, when the systems were bistable, no transitions between attractors were observed, and no new attractors emerged. Consequently, this study represents the inherent complexity and uncertainty in the behavior of networks composed of extreme multistable systems, which can help grasp the dynamics of such systems and their responses to coupling. Providing the multistability conditions as a theorem will be considered in the future works.

Declaration of competing interest

The authors declare that they have no known competing financial interests or personal relationships that could have appeared to influence the work reported in this paper.

Acknowledgments

M.P. is supported by the Slovenian Research and Innovation Agency (Javna agencija za znanstvenoraziskovalno in inovacijsko dejavnost Republike Slovenije) (Grant Nos. P1-0403 and N1-0232). The work is also partially funded by Centre for Nonlinear Systems, Chennai Institute of Technology, India vide funding number CIT/CNS/2023/RP/010.

References

[1] K. Li, Z. Ma, Z. Jia, M. Small, X. Fu, Interplay between collective behavior and spreading dynamics on complex networks, Chaos 22 (4) (2012) http://dx.doi.org/10.1063/1.4766677.
[2] S. Boccaletti, V. Latora, Y. Moreno, M. Chavez, D.-U. Hwang, Complex networks: Structure and dynamics, Phys. Rep. 424 (4–5) (2006) 175–308, http://dx.doi.org/10.1016/j.physrep.2005.10.009.
[3] A.J. O'malley, P.V. Marsden, The analysis of social networks, Health Serv. Outcomes Res. Methodol. 8 (2008) 222–269, http://dx.doi.org/10.1007/s10742-008-0041-z.
[4] M. Girvan, M.E. Newman, Community structure in social and biological networks, Proc. Natl. Acad. Sci. 99 (12) (2002) 7821–7826, http://dx.doi.org/10.1073/pnas.12265379.
[5] J. Kleinberg, The convergence of social and technological networks, Commun. ACM 51 (11) (2008) 66–72, http://dx.doi.org/10.1145/1400214.1400232.
[6] A. Arenas, A. Díaz-Guilera, J. Kurths, Y. Moreno, C. Zhou, Synchronization in complex networks, Phys. Rep. 469 (3) (2008) 93–153, http://dx.doi.org/10.1016/j.physrep.2008.09.002.
[7] F. Sorrentino, L.M. Pecora, A.M. Hagerstrom, T.E. Murphy, R. Roy, Complete characterization of the stability of cluster synchronization in complex dynamical networks, Sci. Adv. 2 (4) (2016) e1501737, http://dx.doi.org/10.1126/sciadv.1501737.
[8] F. Parastesh, S. Jafari, H. Azarnoush, Z. Shahriari, Z. Wang, S. Boccaletti, M. Perc, Chimeras, Phys. Rep. 898 (2021) 1–114, http://dx.doi.org/10.1016/j.physrep.2020.10.003.
[9] B. Yan, F. Parastesh, S. He, K. Rajagopal, S. Jafari, M. Perc, Interlayer and intralayer synchronization in multiplex fractional-order neuronal networks, Fractals 30 (10) (2022) 2240194, http://dx.doi.org/10.1142/S0218348X22401946.
[10] S.N. Chowdhury, S. Majhi, M. Ozer, D. Ghosh, M. Perc, Synchronization to extreme events in moving agents, New J. Phys. 21 (7) (2019) 073048, http://dx.doi.org/10.1088/1367-2630/ab2a1f.
[11] C.H. Totz, S. Olmi, E. Schöll, Control of synchronization in two-layer power grids, Phys. Rev. E 102 (2) (2020) 022311, http://dx.doi.org/10.1103/PhysRevE.102.022311.
[12] T. Dahms, J. Lehnert, E. Schöll, Cluster and group synchronization in delay-coupled networks, Phys. Rev. E 86 (1) (2012) 016202, http://dx.doi.org/10.1103/PhysRevE.86.016202.
[13] R.V. Mendes, Multistability in dynamical systems, in: Dynamical Systems: From Crystal to Chaos, World Scientific, 2000, pp. 105–113.
[14] C. Hens, R. Banerjee, U. Feudel, S. Dana, How to obtain extreme multistability in coupled dynamical systems, Phys. Rev. E 85 (3) (2012) 035202, http://dx.doi.org/10.1103/PhysRevE.85.035202.
[15] H. Bao, M. Hua, J. Ma, M. Chen, B. Bao, Offset-control plane coexisting behaviors in two-memristor-based hopfield neural network, IEEE Trans. Ind. Electron. 70 (10) (2022) 10526–10535, http://dx.doi.org/10.1109/TIE.2022.3222607.
[16] J.S. Kelso, Multistability and metastability: understanding dynamic coordination in the brain, Philos. Trans. R. Soc. B 367 (1591) (2012) 906–918, http://dx.doi.org/10.1098/rstb.2011.0351.
[17] Z.T. Njitacke, M.E. Sone, T.F. Fozin, N. Tsafack, G.D. Leutcho, C.T. Tchapga, Control of multistability with selection of chaotic attractor: application to image encryption, Eur. Phys. J. Special Top. 230 (7–8) (2021) 1839–1854, http://dx.doi.org/10.1140/epjs/s11734-021-00137-6.
[18] G. Li, J. Duan, D. Li, N. Wang, Generation mechanisms of strange nonchaotic attractors and multistable dynamics in a class of nonlinear economic systems, Nonlinear Dynam. 111 (11) (2023) 10617–10627, http://dx.doi.org/10.1007/s11071-023-08382-1.
[19] M. Chen, M. Sun, B. Bao, H. Wu, Q. Xu, J. Wang, Controlling extreme multistability of memristor emulator-based dynamical circuit in flux–charge domain, Nonlinear Dynam. 91 (2018) 1395–1412, http://dx.doi.org/10.1007/s11071-017-3952-9.
[20] B.-C. Bao, Q. Xu, H. Bao, M. Chen, Extreme multistability in a memristive circuit, Electron. Lett. 52 (12) (2016) 1008–1010, http://dx.doi.org/10.1049/el.2016.0563.
[21] R.E. Gutierrez, J.M. Rosário, J. Tenreiro Machado, et al., Fractional order calculus: basic concepts and engineering applications, Math. Probl. Eng. 2010 (2010) 375858, http://dx.doi.org/10.1155/2010/375858.
[22] S. He, H. Wang, K. Sun, Solutions and memory effect of fractional–order chaotic system: A review, Chin. Phys. B 31 (6) (2022) 060501, http://dx.doi.org/10.1088/1674-1056/ac43ae.
[23] Y. Wang, G. Zhao, A comparative study of fractional-order models for lithium-ion batteries using runge kutta optimizer and electrochemical impedance spectroscopy, Control Eng. Pract. 133 (2023) 105451, http://dx.doi.org/10.1016/j.conengprac.2023.105451.
[24] M. Farman, A. Akgül, M.U. Saleem, S. Imtiaz, A. Ahmad, Dynamical behaviour of fractional–order finance system, Pramana 94 (2020) 1–10, http://dx.doi.org/10.1007/s12043-020-02030-8.
[25] L.V.C. Hoan, M.A. Akinlar, M. Inc, J. Gómez-Aguilar, Y.-M. Chu, B. Almohsen, A new fractional–order compartmental disease model, Alexandria Eng. J. 59 (5) (2020) 3187–3196, http://dx.doi.org/10.1016/j.aej.2020.07.040.
[26] K. Rajagopal, N. Hasanzadeh, F. Parastesh, I.I. Hamarash, S. Jafari, I. Hussain, A fractional–order model for the novel coronavirus (COVID-19) outbreak, Nonlinear Dynam. 101 (2020) 711–718, http://dx.doi.org/10.1007/s11071-020-05757-6.
[27] S. He, S. Banerjee, K. Sun, Complex dynamics and multiple coexisting attractors in a fractional-order microscopic chemical system, Eur. Phys. J. Special Top. 228 (2019) 195–207, http://dx.doi.org/10.1140/epjst/e2019-800166-y.
[28] S. Gu, S. He, H. Wang, B. Du, Analysis of three types of initial offset-boosting behavior for a new fractional-order dynamical system, Chaos Solitons Fractals 143 (2021) 110613, http://dx.doi.org/10.1016/j.chaos.2020.110613.
[29] G.-C. Wu, T.-T. Song, S. Wang, Caputo–Hadamard fractional differential equations on time scales: Numerical scheme, asymptotic stability, and chaos, Chaos 32 (9) (2022) 093143, http://dx.doi.org/10.1063/5.0098375.
[30] C. Li, G. Peng, Chaos in Chen's system with a fractional order, Chaos Solitons Fractals 22 (2) (2004) 443–450, http://dx.doi.org/10.1016/j.chaos.2004.02.013.
[31] W. Deng, C. Li, Synchronization of chaotic fractional Chen system, J. Phys. Soc. Japan 74 (6) (2005) 1645–1648, http://dx.doi.org/10.1143/jpsj.74.1645.
[32] J.-L. Wei, G.-C. Wu, B.-Q. Liu, J.J. Nieto, An optimal neural network design for fractional deep learning of logistic growth, Neural Comput. Appl. 35 (15) (2023) 10837–10846, http://dx.doi.org/10.1007/s00521-023-08268-8.
[33] G.-C. Wu, J.-L. Wei, T.-C. Xia, Multi–layer neural networks for data–driven learning of fractional difference equations' stability, periodicity and chaos, Physica D 457 (2023) 133980, http://dx.doi.org/10.1016/j.physd.2023.133980.
[34] Z. Deng, C. Wang, H. Lin, Y. Sun, A memristive spiking neural network circuit with selective supervised attention algorithm, IEEE Trans. Comput. Aided Des. Integr. Circuits Syst. 42 (8) (2023) 2604–2617, http://dx.doi.org/10.1109/TCAD.2022.3228896.

[35] O.I. Abiodun, A. Jantan, A.E. Omolara, K.V. Dada, A.M. Umar, O.U. Linus, H. Arshad, A.A. Kazaure, U. Gana, M.U. Kiru, Comprehensive review of artificial neural network applications to pattern recognition, IEEE Access 7 (2019) 158820–158846, http://dx.doi.org/10.1109/ACCESS.2019.2945545.
[36] H.-J. Yoo, Deep convolution neural networks in computer vision: A review, IEIE Trans. Smart Process. Comput. 4 (1) (2015) 35–43, http://dx.doi.org/10.5573/IEIESPC.2015.4.1.035.
[37] B. Bao, C. Chen, H. Bao, X. Zhang, Q. Xu, M. Chen, Dynamical effects of neuron activation gradient on hopfield neural network: Numerical analyses and hardware experiments, Int. J. Bifurcation Chaos 29 (04) (2019) 1930010, http://dx.doi.org/10.1142/S0218127419300106.
[38] Q. Xu, S. Ding, H. Bao, B. Chen, B. Bao, Activation function effects and simplified implementation for hopfield neural network, J. Circuits Syst. Comput. 32 (18) (2023) 2350313, http://dx.doi.org/10.1142/S0218126623503139.
[39] H. Lin, C. Wang, F. Yu, Q. Hong, C. Xu, Y. Sun, A triple-memristor hopfield neural network with space multi-structure attractors and space initial-offset behaviors, IEEE Trans. Comput. Aided Des. Integr. Circuits Syst. 42 (12) (2023) 4948–4958, http://dx.doi.org/10.1109/TCAD.2023.3287760.
[40] M. Hua, H. Bao, H. Wu, Q. Xu, B. Bao, A single neuron model with memristive synaptic weight, Chinese J. Phys. 76 (2022) 217–227, http://dx.doi.org/10.1016/j.cjph.2021.10.042.
[41] B. Sriram, F. Parastesh, H. Natiq, K. Rajagopal, S. Jafari, Super extreme multistability in a two-dimensional fractional-order forced neural model, Eur. Phys. J. Special Top. 232 (2023) 2559–2565, http://dx.doi.org/10.1140/epjs/s11734-023-00914-5.
[42] K. Diethelm, A.D. Freed, The fracPECE subroutine for the numerical solution of differential equations of fractional order, Forsch. Wiss. Rechn. 1999 (1998) 57–71.
[43] G.A. Gottwald, I. Melbourne, On the implementation of the 0–1 test for chaos, SIAM J. Appl. Dyn. Syst. 8 (1) (2009) 129–145, http://dx.doi.org/10.1137/080718851.
[44] X. Yu, H. Bao, M. Chen, B. Bao, Energy balance via memristor synapse in Morris–Lecar two-neuron network with FPGA implementation, Chaos Solitons Fractals 171 (2023) 113442, http://dx.doi.org/10.1016/j.chaos.2023.113442.